Accepted Manuscript

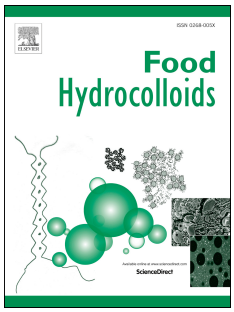

A further study on supramolecular structure changes of waxy maize starch subjected to alkaline treatment by extended-*q* small-angle neutron scattering

Binjia Zhang, Elliot P. Gilbert, Dongling Qiao, Fengwei Xie, David K. Wang, Siming Zhao, Fatang Jiang

PII: S0268-005X(19)30389-3

DOI: https://doi.org/10.1016/j.foodhyd.2019.04.031

Reference: FOOHYD 5060

To appear in: *Food Hydrocolloids*

Received Date: 18 February 2019

Revised Date: 9 April 2019

Accepted Date: 15 April 2019

Please cite this article as: Zhang, B., Gilbert, E.P., Qiao, D., Xie, F., Wang, D.K., Zhao, S., Jiang, F., A further study on supramolecular structure changes of waxy maize starch subjected to alkaline treatment by extended-*q* small-angle neutron scattering, *Food Hydrocolloids* (2019), doi: https://doi.org/10.1016/j.foodhyd.2019.04.031.

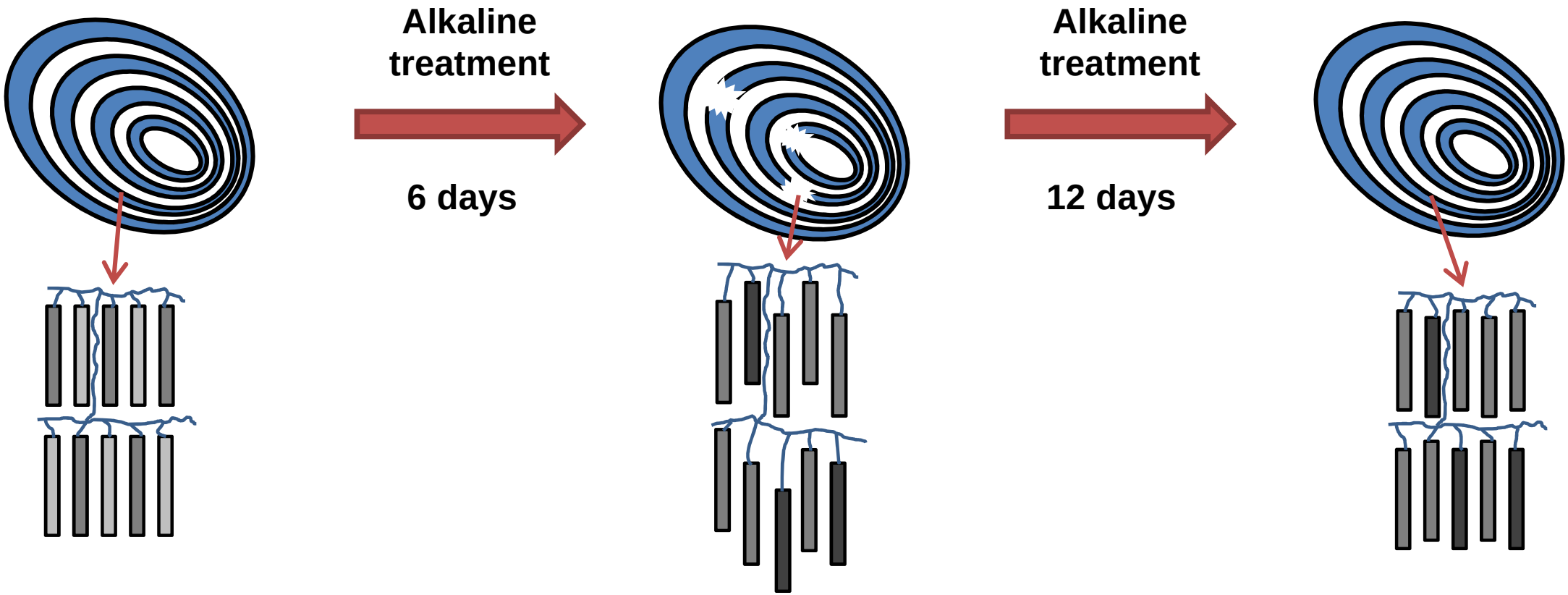

A further study on supramolecular structure changes of waxy maize starch subjected to alkaline treatment by extended-*q* small-angle neutron scattering

Binjia Zhang[a], Elliot P. Gilbert[b,c], Dongling Qiao[d,*], Fengwei Xie[e,f,†], David K. Wang[g], Siming Zhao[a], Fatang Jiang[d]

[a] *Group for Cereals and Oils Processing, Key Laboratory of Environment Correlative Dietology (Ministry of Education), College of Food Science and Technology, Huazhong Agricultural University, Wuhan 430070, China*

[b] *Australian Centre for Neutron Scattering, Australian Nuclear Science and Technology Organisation, Locked Bag 2001, Kirrawee DC, NSW 2232, Australia*

[c] *The Australian Institute for Bioengineering and Nanotechnology, and Queensland Alliance for Agriculture and Food Innovation, The University of Queensland, Brisbane, Qld 4072, Australia*

[d] *Glyn O. Philips Hydrocolloid Research Centre at HBUT, Hubei University of Technology, Wuhan 430068, China*

[e] *International Institute for Nanocomposites Manufacturing (IINM), WMG, University of Warwick, Coventry CV4 7AL, United Kingdom*

[f] *School of Chemical Engineering, The University of Queensland, Brisbane, Qld 4072, Australia*

[g] *School of Chemical and Biomolecular Engineering, The University of Sydney, Darlington, NSW 2006, Australia*

[*] Corresponding Author. Email: qdttkl@163.com (D. Qiao)

[†] Corresponding Author. Emails: d.xie.2@warwick.ac.uk, f.xie@uq.edu.au (F. Xie)

Abstract: Recently, we reported the effect of mild alkaline treatment on the structure and enzymatic hydrolysis of waxy maize starch. Here, we have used extended-*q* small-angle neutron scattering (SANS) to examine the extent to which this treatment causes structural changes on even greater length scales — to yield a complete picture from the nanometre to micron — including on the lamellar distribution and larger-scale structural features of the same starch. For this A-type polymorph starch containing mostly amylopectin, we found the changes caused by NaOH solution treatment (0.1% or 0.5% (w/v)) were confined mainly to double helices and crystallites, whereas the lamellar and supramolecular structures were conserved. Although the overall lamellar ordering was reduced in the 0.5% (w/v) alkaline treatment for 6 days, further treatment until 12 days could restore the overall lamellar ordering. Despite changes in starch double helical order and crystallites, there were minimal changes at larger length scales (*e.g.*, blocklets and growth rings). This combination of methods reveals the extent of structural changes occurring as a result of mild alkaline treatment of waxy maize starch; it also provides insight into the rational design of granular starch products with varied functionality via hydrolytic control.

Keywords: starch; double helices, lamellae; large-scale structure; extended-*q* small-angle neutron scattering; SANS

1 Introduction

Starch, as a storage polysaccharide in green plants such as maize, potato, wheat, and rice (Xie, Zhang, & Wang, 2017), serves as a food ingredient providing energy to humans (Juansang, Puttanlek, Rungsardthong, Puncha-arnon, & Uttapap, 2012). Starch is also relevant for the design of functional foods (Fuentes-Zaragoza et al., 2011), bioactive carriers (Pu, Chen, Li, Xie, Yu, & Li, 2011) and biomaterials (Situ, Li, Liu, & Chen, 2015). There are two starch polymers biosynthesised during plant growth, namely amylose and amylopectin (Liu, Halley, & Gilbert, 2010; Jiang, Gao, Li, & Zhang, 2011). These two polymers can be organized on different scales in the starch granule to construct a multiscale supramolecular system; this system involves the whole granule, growth rings, blocklets, semicrystalline lamellae, crystallites, and double/single helices (Buleon, Colonna, Planchot, & Ball, 1998; Luengwilai & Beckles, 2009; Perez & Bertoft, 2010; Blazek & Gilbert, 2011; Doutch & Gilbert, 2013; Flanagan, Gidley, & Warren, 2015; Zhang et al., 2015). The structures with scales larger than that of lamellae can be loosely termed as ‘large-scale’ structures, including the growth rings and blocklets (Doutch et al., 2013).

The multiscale structural features of starch such as crystallinity, the degree of lamellar ordering, and the bulk density of the granule surface (associated with pores in cereal starches) are crucial in governing starch properties and functions (*e.g.*, thermal behaviours and digestibility) (Lopez-Rubio, Flanagan, Shrestha, Gidley, & Gilbert, 2008b; Liu, Xie, Yu, Chen, & Li, 2009; Blazek & Gilbert, 2010; Xie, Halley, & Avérous, 2012). For instance, a multiscale supramolecular structure with tightly assembled starch chains can weaken the enzyme diffusion and hydrolysis, thus making the digestion rate of untreated starch several times lower than that of cooked starch (Bertoft & Manelius, 1992;

Noda et al., 2008; Blazek et al., 2010). Therefore, revealing the starch multiscale structure using advanced analytical techniques can help in understanding such structure–function relationships.

Small-angle X-ray scattering (SAXS) and small-angle neutron scattering (SANS) are among the most powerful techniques for characterizing the lamellar and large-scale structures of starch (Chanvrier et al., 2007; Lopez-Rubio, Htoon, & Gilbert, 2007; Lopez-Rubio, Flanagan, Gilbert, & Gidley, 2008a; Lopez-Rubio et al., 2008b; Blazek et al., 2010; Blazek et al., 2011; Witt, Doutch, Gilbert, & Gilbert, 2012; Doutch et al., 2013; Bai, Cai, Doutch, Gilbert, & Shi, 2014; Shrestha et al., 2015; Yang et al., 2019a). With these two scattering techniques, it is straightforward to extract information on the supramolecular structural features of starch such as the thickness of semicrystalline lamellae, crystalline and amorphous block dimensions (Cardoso & Westfahl, 2010; Zhang et al., 2014), and the size of blocklets (Doutch et al., 2013).

Alkaline treatment is widely used for the isolation of starches with high yields and purity from agro-products (Han & Hamaker, 2002; Correia & Beirão-da-Costa, 2012) and for the production of a wide variety of starch-based foods such as tortillas, yellow alkaline noodles, and dumplings (Campus-Baypoli, Rosas-Burgos, Torres-Chavez, Ramírez-Wong, & Serna-Saldivar, 1999; Lai, Karim, Norziah, & Seow, 2002). Alkalis, such as sodium hydroxide and sodium carbonate, can impart foods with typical aroma and flavour as well as a firm and elastic texture (Karim, Nadiha, Chen, Phuah, Chui, & Fazilah, 2008). It has been shown that alkaline treatment can alter the molecular structure (amylose content), hierarchical structures (granule morphology, lamellae, crystallites, and short-range order), and properties (*e.g.*, swelling, pasting, rheological, thermal, and digestion behaviours) of various starches (*e.g.*, corn, rice, potato, sago, and pea) (Lai et al., 2002; Cardoso, Putaux, Samios, & da Silveira, 2007; Méndez-Montealvo, Trejo-Espino, Paredes-López, &

Bello-Pérez, 2007; Karim et al., 2008; Thys, Westfahl, Norea, Marczak, Silveira, & Cardoso, 2008; Nor Nadiha, Fazilah, Bhat, & Karim, 2010; Wang & Copeland, 2012; Cai et al., 2014; Jiang et al., 2014; Wang, Luo, Zhang, Zhang, He, & Wang, 2014; Qiao et al., 2016). However, how alkaline conditions (especially mild) change the lamellar distribution and large-scale characteristics is not well defined. Moreover, as the susceptibility of starch to alkaline treatment greatly depends on its native granule architecture and molecular structure (Nor Nadiha et al., 2010; Jiang et al., 2014), it is worth studying how alkaline treatment could have varied effects on a variety of cultivars. Our previous study (Qiao et al., 2017) has shown that mild alkaline treatment (0.1% and 0.5% NaOH, w/v) can effectively alter the digestion behaviour of waxy maize starch. However, how alkaline treatment alters the supramolecular structure of an A-type polymorphic starch (the mechanism) is still not fully understood. To answer this question, an investigation of changes occurring on multiple and relevant length scales is essential. To this end, we have used an extended-*q* SANS to interrogate the lamellar distribution and large-scale features of starch spanning scales up to the micron and their evolution under alkaline treatment. Note that SAXS and SANS are complementary methods. SAXS is sensitive to electron density differences, whereas SANS is sensitive to differences in neutron scattering length density (SLD) (a nuclear property); the latter can be manipulated through solvent contrast variation and selective deuteration, for example. In the current case, neutron scattering has been employed to enable access to a wide *q* range to examine the hierarchical structures exhibited by starch; the latter is readily available on the QUOKKA SANS instrument (Gilbert, Schulz, & Noakes, 2006; Wood et al., 2018). Neutron focussing, enabling access to scattering vectors down to about 0.00045 $Å^{-1}$, has also been used to simultaneously characterize the lamellar and large-scale structure of alkali-treated starch from the nanoscale to the micron-scale. A modified method was established to

fit the SANS data comprising a Gaussian-plus-Lorentzian peak function for the lamellar peak scattering, and a unified model (a Guinier function plus a power-law function) for larger length scales. With this method, the semicrystalline lamellae have been found to be distributed in a narrow range; moreover, the large-scale information related to blocklets and growth rings can be revealed.

2 Materials and methods

2.1 Materials

The starch used in this work was waxy maize starch commercially available from Penford Australia Pty Ltd. (Lane Cove, NSW, Australia). The amylose:amylopectin ratio of this starch was *ca*. 3:97, as determined using the iodine colourimetric method (Tan, Flanagan, Halley, Whittaker, & Gidley, 2007). The moisture content (*ca*. 13.6%) was measured using an MA35 moisture analyser (Sartorius Stedim Biotech GmbH, Germany). All chemicals (including sodium hydroxide, sodium azide, and ethanol) were of analytical grade and were provided by Tianjin Kemeou Chemical Reagent Co., Ltd. (Tianjin, China).

2.2 Alkaline treatment

Although a concentrated alkali solution can quickly and effectively disrupt the starch structure, it may also result in the degradation of starch molecules (Han & Lim, 2004) due to the β-elimination of reducing semi-acetal groups. In this work, NaOH aqueous solutions of 0.1% (w/v) and 0.5% (w/v) concentrations were employed for the treatment of the starch for different times (6 and 12 days).

Such mild alkali solutions were selected as they are typical for the processing of starch and starch-based foods where the modest alteration of the starch multiscale structure without degrading or dissolving starch molecules is desirable (Nor Nadiha et al., 2010; Praznik, Buksa, Ziobro, Gambuś, & Nowotna, 2012; Wang et al., 2012; Cai et al., 2014; Jiang et al., 2014).

Specifically, NaOH aqueous solutions of 0.1% (w/v) or 0.5% (w/v) concentration were prepared with 0.1% (w/v) sodium azide as a chemical preservative. About 10 g of the starch was added to 150 mL of the alkali solutions. The starch slurries were then placed at 35 °C for different treatment days (6 or 12), accompanied by intermittent shaking to effectively re-suspend the starch. Afterwards, each alkali-treated starch sample was washed using deionized water and then 95% ethanol (Wang et al., 2012; Jiang et al., 2014), followed by centrifugation for at least 3 times until a neutral starch slurry was acquired. The starch sediments were dried in an oven at 35 °C for 48 h and then were placed into zip-lock bags for further use.

In the following, codes such as “S-0.1-6” will be used, in which “S” denotes the waxy maize starch, “0.1” indicates the alkali concentration being 0.1% (w/v), and “6” means the days of treatment. In addition, a code of only “S” in the figures and tables indicates the native starch without any treatment.

2.3 Extended-*q* small-angle neutron scattering (SANS)

SANS measurements, extended to an ultra-small angle (q = *ca*. 0.00045 Å^{-1}), were performed on the 40-m QUOKKA instrument at the OPAL reactor (Sydney, Australia) (Gilbert et al., 2006; Wood et al., 2018). The sample aperture diameters were of 50 and 7.5 mm, respectively. Three instrument

configurations, with sample-to-detector distances of 1.3, 8.0 and 20.0 m at a wavelength (λ) of 5.0 Å and a fourth with wavelength 8.1 Å, and 10% wavelength resolution, were used to provide a continuous q range of *ca*. 0.00045 to 0.70 Å^{-1}, where q is the scattering vector defined as $q = 4\pi\sin\theta/\lambda$ (2θ is the scattering angle (°)). The instrumental resolution, Δq, at the lamellar peak (0.06 to 0.07 Å^{-1}) is 0.003 Å^{-1}. Note that q_{min} is almost one order of magnitude lower than that used in SAXS ($0.0020 < q < 0.20$ Å^{-1}) previously (Qiao et al., 2017) enabling access to larger size range. The starch slurries in heavy water with a starch concentration of 10 wt.% were loaded into demountable cells with quartz windows which, in turn, were placed in a multi-position sample tumbler to prevent sample sedimentation; the scattering of pure heavy water within a quartz cell of 1 mm thickness was used as a background.

2.4 Reduction of SANS data

The resultant SANS data sets were reduced, normalised, and radially averaged using a package of macros in Igor software modified to accept *HDF5* data files from QUOKKA (Blazek et al., 2010). The scattering curves are plotted as a function of absolute (SANS) intensity, I (cm^{-1}), versus q (Å^{-1}).

2.5 Fitting of SANS data

The extended-q SANS data covering q values of *ca*. 0.00045 to 0.20 Å^{-1} were fitted in Origin 8 software (OriginLab. Inc., USA). Curve fitting was conducted iteratively; for each iteration, the fitting coefficients were refined to minimise chi-squared via a nonlinear, least-squares refinement procedure. As detailed in **Section 3.3**, the scattering data were fitted with a unified model including

two power-law regimes (Doutch et al., 2013; Zhang et al., 2015) plus a Gaussian-plus-Lorentzian peak function to describe the lamellar peak range (*ca*. 0.015 to 0.20 $Å^{-1}$). Data are expressed as means ± standard deviations (SD).

3 Results and discussion

3.1 Short- and long-range structural changes of alkali-treated starch (previous study)

In our previous paper (Qiao et al., 2017), we reported the structure and *in-vitro* digestion behaviour of waxy maize starch under the same alkaline treatment conditions. Alkali concentration has been shown to largely influence the short-range structures (double helix and crystallite order) of waxy maize starch (**Table 1**) (Qiao et al., 2017). Using differential scanning calorimetry (DSC), we found the 0.1% (w/v) alkaline treatment could decrease the onset temperature (T_o), increase the conclusion temperature (T_c), and slightly reduce the enthalpy (ΔH) of gelatinisation. X-ray diffraction (XRD) data indicated a slightly reduced degree of crystallinity (X_c). Similar changes in DSC results were observed for other types of starch (Méndez-Montealvo et al., 2007; Nor Nadiha et al., 2010; Wang et al., 2012; Cai et al., 2014; Wang et al., 2014). For waxy maize starch with A-type crystallites, the only endothermic peak represents an overlap of the transitions from smectic to isotropic phase and the helix–coil transition associated with the unwinding of amylopectin double helices (starch molecular order) (Waigh, Gidley, Komanshek, & Donald, 2000a). It was proposed that the 0.1% (w/v) alkaline treatment could weaken the hydrogen-bonding interactions between double helices, disrupt some double helices, and increase the degree of perfection of some double

184 helices. With a stronger alkaline (0.5% NaOH, w/v) treatment, the starch displayed increased T_o and
185 T_c and decreased ΔH and X_c. In this regard, the 0.5% (w/v) NaOH solution could effectively disrupt
186 some starch double helices especially those with flaws or a lower degree of perfection and increase
187 the level of perfection for some existing starch double helices.
188
189 **Table 1** Crystalline and thermal parameters of native and alkali-treated starch samples[A].
190 Reproduced from Ref. (Qiao et al., 2017), Copyright (2017), with permission from Elsevier.

	S	S-0.1-6	S-0.1-12	S-0.5-6	S-0.5-12
X_c (%)	49.21±0.68 ^{a}	47.31±0.75 ^{b}	44.70±1.02 ^{c}	39.62±1.10 ^{e}	42.52±0.96 ^{d}
T_o (°C)	72.31±0.20 ^{b}	68.96±0.35 ^{c}	67.95±0.19 ^{d}	77.35±0.23 ^{a}	77.17±0.37 ^{a}
T_p (°C)	78.57±0.15 ^{c}	75.98±0.22 ^{d}	75.38±0.16 ^{e}	81.95±0.26 ^{a}	81.27±0.18 ^{b}
T_c (°C)	86.14±0.32 ^{d}	89.11±0.24 ^{c}	89.88±0.38 ^{b}	90.06±0.43 ^{a}	89.73±0.23 ^{ab}
ΔT (°C)	13.83±0.12 ^{c}	20.15±0.11 ^{b}	21.93±0.19 ^{a}	12.71±0.20 ^{d}	12.56±0.14 ^{e}
ΔH (J/g)	15.42±0.16 ^{a}	15.12±0.21 ^{b}	14.28±0.38 ^{c}	10.55±0.26 ^{e}	11.52±0.22 ^{d}

191 [A] Parameter obtained by XRD: X_c, relative crystallinity. Thermal transition parameters measured by DSC: T_o, onset temperature;
192 T_p, peak temperature; T_c, conclusion temperature; ΔT ($T_c - T_o$), transition temperature range; ΔH, transition enthalpy. Values are
193 means of three determinations ($n = 3$) values. Different letters within a row mean a significant difference ($P < 0.05$). All the
194 values are represented in average ± standard deviation.
195

196 ### 3.2 Features of extended-*q* SANS data

197 **Fig. 1A** presents the extended-*q* SANS patterns on a logarithmic scale of the starch subjected to
198 the 0.1% (w/v) or 0.5% (w/v) alkaline treatment for different days (6 or 12 days). All starch samples
199 had a typical scattering peak at about 0.065 $Å^{-1}$, ascribed to the semicrystalline lamellar structure
200 within the starch granule (Zhang et al., 2017a). This peak may be somewhat weakened by the
201 stronger alkaline solution resulting from the alkali-induced disruption of semicrystalline lamellae. As
202 revealed by the Lorentz-corrected (I^*q^2 *vs.* q) SANS profiles included in **Fig. 1B**, there is an
203 inflection region between the two regimes. A randomly-oriented, dilute system of lamellae would
204 give rise to a q^{-2} dependence (Doutch et al., 2013). Here, the power-law dependence for the starch
205 lamellar peak regime extends to *ca.* 0.015 $Å^{-1}$ (the inflection region). Below this regime, the q
206 dependence of starch neutron scattering changes to q^{-3} or q^{-4}, which is consistent with interfacial
207 scattering; such interfacial scattering can be observed more clearly on a Porod (I^*q^4 *vs.* q) SANS plot
208 (**Fig. 1C**).
209

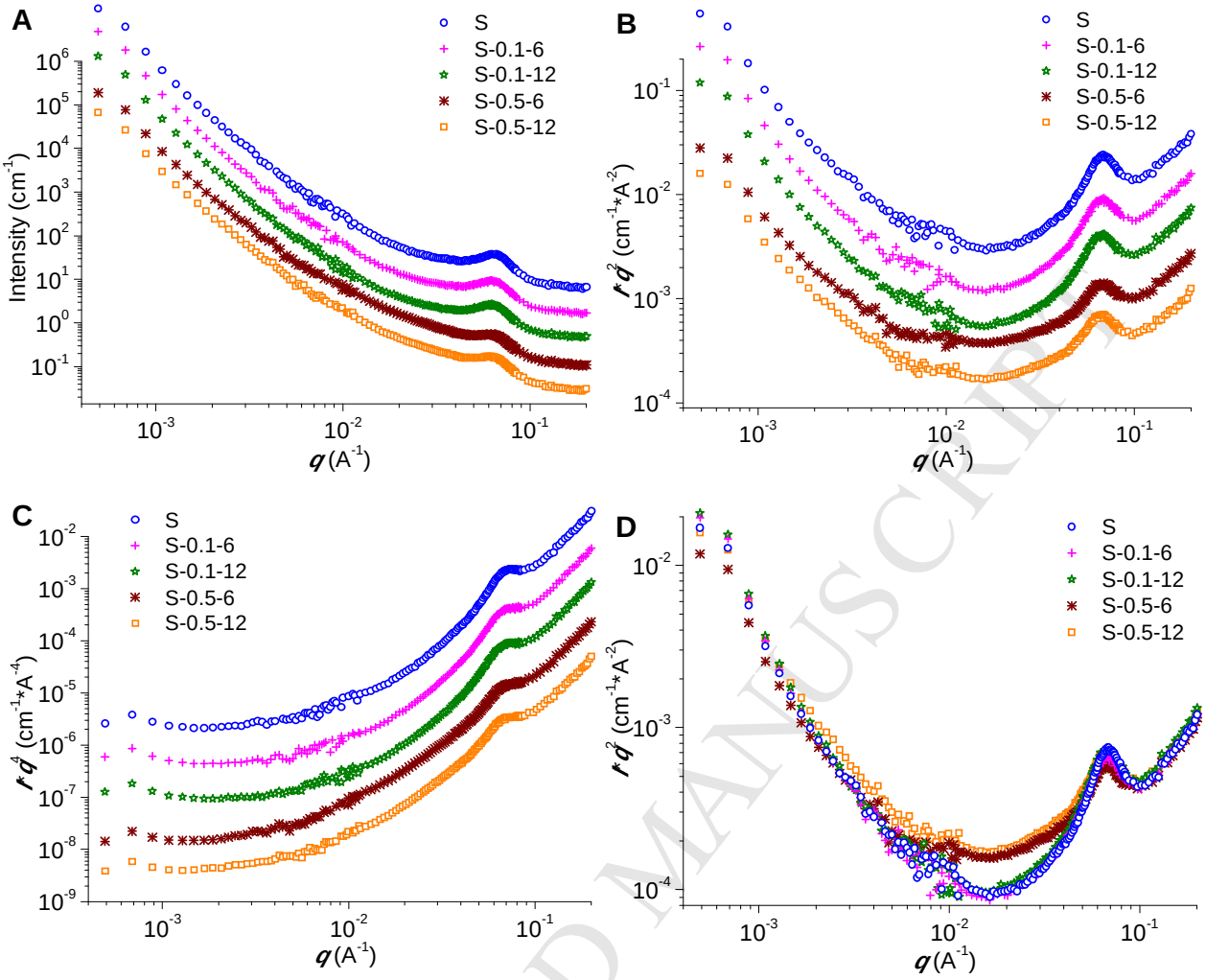

Fig. 1 Double-logarithm (A), Lorentz-corrected ($I*q^2$ *vs.* q) (B and D), and Porod ($I*q^4$ *vs.* q) (C) extended-q SANS patterns for waxy maize starch subjected to 0.1% (w/v) NaOH or 0.5% (w/v) NaOH solution treatment for 6 or 12 days. In A-C, data have been shifted vertically for clarity; in D, data are directly overlaid. In the latter, differences in SANS at q values below the lamellar peak can be clearly observed.

3.3 Data fitting

The fitting curves for the extended-q SANS data are shown in **Fig. 2**. For the power-law regime, a unified model **Eq. (1)** (Beaucage, 2004; Zhang et al., 2017b) was used to fit the relevant scattering data.

$$I(q) = G\exp\left(-\frac{R_g^2 q^2}{3}\right) + C\left(\frac{\left(erf\left(\frac{qR_g}{\sqrt{6}}\right)\right)^3}{q}\right)^{\delta} \quad (1)$$

In this equation, G is the prefactor of the Guinier function corresponding to a radius R_g; C and δ are the prefactor and the exponent of the power-law function, respectively.

For the lamellar peak regime of 0.015–0.20 Å^{-1}, an additional Gaussian-plus-Lorentzian function (**Eq. (2)**) were used to fit the peak scattering $I_{peak}(q)$.

$$I_{peak}(q) = B + f\frac{A\sqrt{\ln 4}}{w\sqrt{\frac{\pi}{2}}}\exp\left(-\frac{2\ln 4(q-q_{peak})^2}{W^2}\right) + (1-f)\frac{2A}{\pi}\times\frac{2W}{4(q-q_{peak})^2 + W^2} \quad (2)$$

In this equation, the first term B is the scattering background; the second and third terms are the Gaussian and Lorentzian functions, respectively, describing the lamellar peak centred on about 0.065 Å^{-1}; f is the prefactor for the peak. In the Gaussian and Lorentzian functions, A is the peak area, W (Å^{-1}) is the peak full width at half maximum (FWHM) in reciprocal space, and q_{peak} (Å^{-1}) is the peak centre position. **Fig. 2** shows satisfactory fitting results for the scattering data.

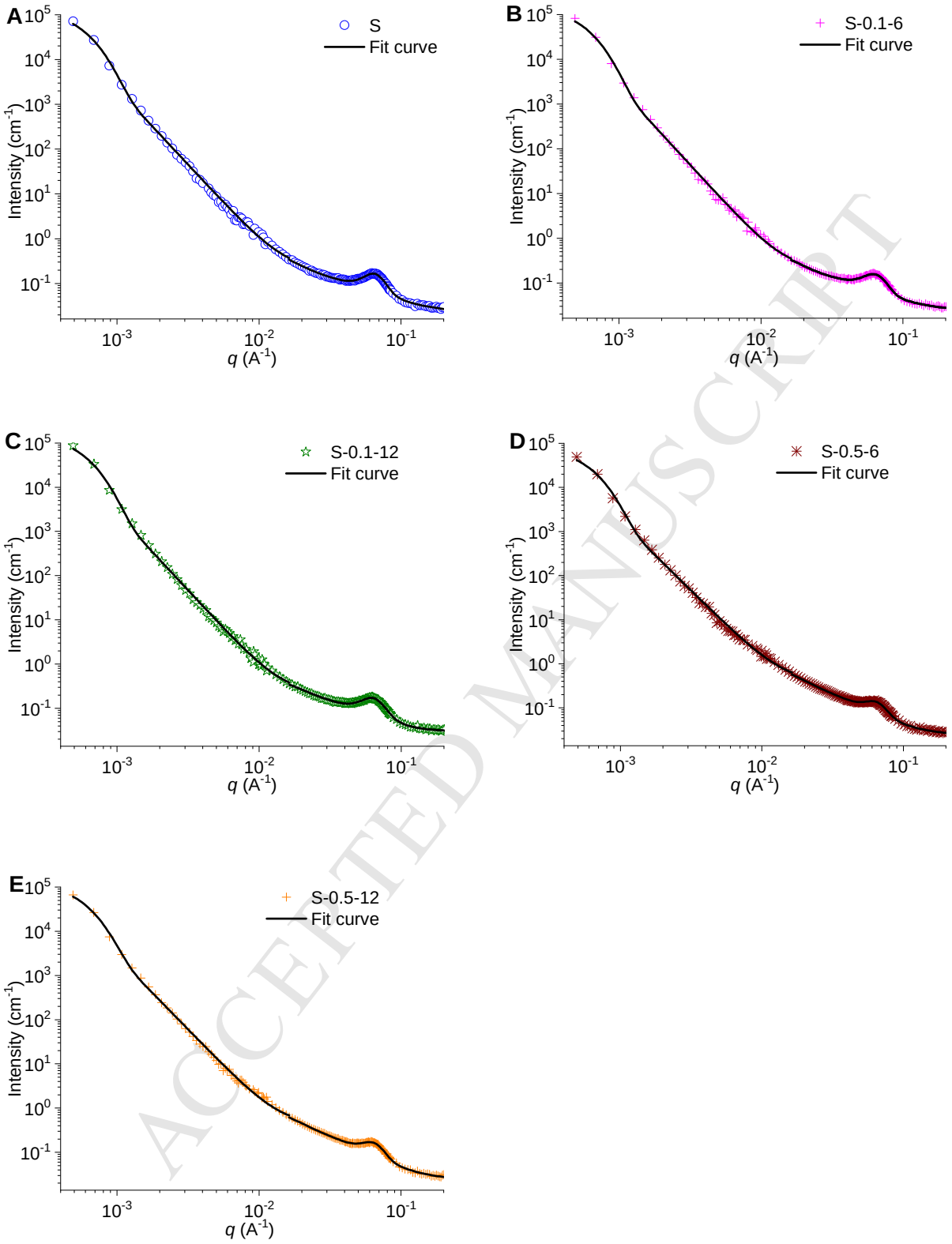

Fig. 2 Extended-*q* SANS patterns and their fitted curves of waxy maize starch subjected to 0.1% (w/v) or 0.5% (w/v) NaOH treatment for 6 or 12 days.

3.4 Lamellar thickness distribution

Fig. 3 illustrates the SANS data (including the scattering from the background, power-law, and lamellae) in the lamellar peak regime (0.015 to 0.20 $Å^{-1}$) and the fitted lamellar peaks (the Gaussian-plus-Lorentzian scattering in **Eq. (2)**) for the untreated and alkali-treated starches. The starches displayed a semicrystalline lamellar peak in the range of *ca.* 0.03 to 0.10 $Å^{-1}$, corresponding to a lamellar distribution with mean thickness (d_{ave}) of *ca*. 9.70–10.00 nm (see **Fig. 4**).

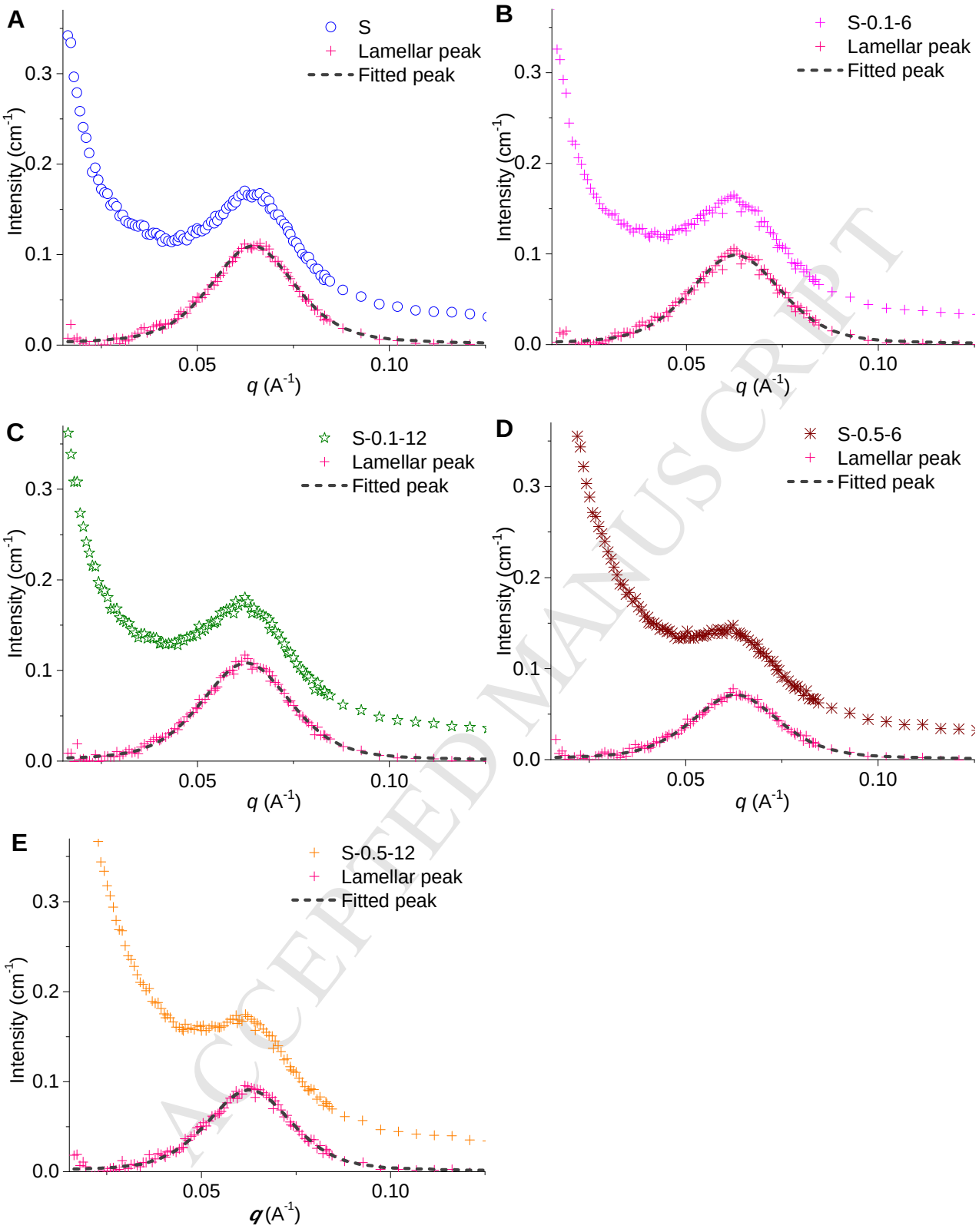

Fig. 3 SANS patterns in the lamellar scattering range, and their fitted lamellar peaks, for waxy maize starch subjected to 0.1% (w/v) NaOH or 0.5% (w/v) NaOH solution treatment for 6 or 12 days.

Table 2 shows the fitted peak positions (q_{peak}) and the FWHMs in reciprocal space (W) of lamellar peak for different starch samples. The peak position was used to calculate the average thickness (d_{ave}) of semicrystalline lamellae according to the Woolf-Bragg equation, $d_{ave} = 2\pi/q_{peak}$. Based on **Eq. (3)**, the associated reciprocal of the space value (W in **Table 2**), W_{real}, is positively related to the thickness distribution width, or equivalently, the lamellar polydispersity, of semicrystalline lamellae based on **Eq. (3)** (Cardoso et al., 2010; Witt et al., 2012).

$$W_{real} = \frac{2\pi W}{q_{peak}^2} \quad (3)$$

The d_{ave} and W_{real} values for different starch samples are illustrated in **Fig. 4**. For the untreated, native starch, d_{ave} was about 9.70 nm and W_{real} about 3.90 nm. Both the 0.1% (w/v) and 0.5% (w/v) alkaline treatments slightly increased d_{ave} to similar extents while the 0.1% (w/v) alkaline solution caused a greater increase in W_{real}. On the other hand, a longer treatment time did not appear to change d_{ave} or W_{real} further.

271 **Table 2** Fitted parameters of the lamellar peak SANS data for waxy maize starch before and after 0.1%

272 (w/v) or 0.5% (w/v) NaOH solution treatment for 6 or 12 days [a]

	S	S-0.1-6	S-0.1-12	S-0.5-6	S-0.5-12
A (Å^{-1} cm^{-1})	0.0027±0.0001	0.0027±0.0001	0.0029±0.0001	0.0018±0.0001	0.0023±0.0001
W (Å^{-1})	0.0264±0.0006	0.0281±0.0009	0.0276±0.0007	0.0269±0.0008	0.0266±0.0008
q_{peak} (Å^{-1})	0.0645±0.0001	0.0628±0.0002	0.0627±0.0002	0.0629±0.0002	0.0627±0.0002
B (cm^{-1})	0.021±0.002	0.022±0.002	0.025±0.002	0.023±0.001	0.022±0.001
f	0.59±0.10	0.71±0.13	0.67±0.10	0.62±0.11	0.67±0.12
Chi^2	1.98	1.98	1.98	1.98	1.98

273 [a] q values used for fitting based on **Eq. (2)**: 0.015 to 0.20 Å^{-1}. The resultant parameters: A, area of the lamellar peak; W, full

274 width at half maximum (FWHM) in reciprocal space; q_{peak}, position of the lamellar peak; B, scattering background; f, prefactor

275 for the lamellar peak function. All the values are represented in average ± standard deviation.

276

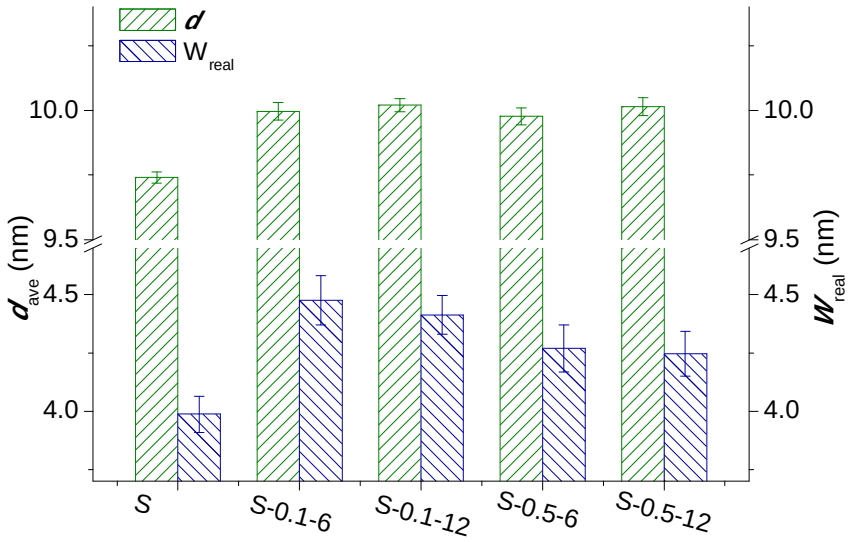

277

278 **Fig. 4** Average semicrystalline lamellar thickness (d_{ave}) (A) and width of distribution (W_{real}) (B) for
279 waxy maize starch subjected to 0.1% (w/v) NaOH or 0.5% (w/v) NaOH solution treatment for 6 or 12
280 days.

281

282 **Table 2** also records the fitted lamellar peak area (*A*), which can be positively correlated with the
283 degree of lamellar ordering (Pikus, 2005; Wang, Wang, Li, Chen, & Zhang, 2017). The 0.1% (w/v)
284 alkaline treatment did not change *A* even after 12 days. In contrast, *A* was reduced by 0.5% (w/v)
285 NaOH solution, and this reduction was even greater for 6 days than for 12 days. Our previous SAXS
286 data (Qiao et al., 2017) indicates that the thickness of crystalline lamellae (d_c) slightly increased and
287 that of amorphous lamellae (d_a) marginally decreased by alkaline treatment. In an earlier study (Qiao
288 et al., 2016), 0.5% (w/v) alkaline treatment of regular maize starch, which is also an A-type
289 polymorphic starch, resulted in a similar increase in d_c while the decrease in d_a was less apparent. In
290 contrast, high-amylose maize starch Gelose 50 (B-type) exhibited increases in both d_c and d_a (Qiao et
291 al., 2016). For other starches subjected to alkaline treatment, a reduction in amylose content has
292 generally been reported (Karim et al., 2008; Nor Nadiha et al., 2010; Wang et al., 2012; Cai et al.,

2014; Jiang et al., 2014). In particular, Cai et al. (2014) reported that for a high-amylose rice starch (C-type), 0.4% NaOH treatment resulted in leaching of amylose from starch granules, which was accompanied by changes in granule morphology and electron density between crystalline and amorphous lamellae. In our case here, we observed only slight changes in d_c and d_a, which may due to the very low amylose content in waxy maize starch. Besides, the amorphous lamellae are normally thought to include the branching points of the amylopectin macromolecules. The decreases in d_a due to mild alkali treatment may arise from either a physical process, for example, the rearrangement of branching points, or a chemical process due to cleavage/hydrolysis of these branching points or, indeed, a combination thereof. On the other hand, the changes to crystalline lamellae were accompanied by the reduced crystallinity and degree of molecular ordering (**Table 1**). When the 0.1% (w/v) alkaline solution was used, any changes to the molecular order and crystallites within crystalline lamellae did not cause significant variation to the overall lamellar ordering (as reflected by an unchanged *A*). Nevertheless, a prominent decrease in *A* was observed for S-0.5-6, indicating the stronger alkaline solution could disrupt the overall lamellar ordering to some extent. This disruption of the lamellar ordering was accompanied by (or should result from) the misalignment of starch double helices (a crystalline smectic–nematic transition), the disruption of less-stable double helices, and the rearrangement of double helices with high degrees of perfection (as reflected by increased T_o and T_c, see **Table 1**). Interestingly, S-0.5-6 presents lower *A* than S-0.5-12, which may indicate that the disruption of the overall lamellae by strong alkaline treatment was temporary and a longer time of such a treatment could restore the lamellar ordering to some extent although more detailed studies are required to confirm this.

Irrespective of the alkali concentration and treatment time, the four treated samples exhibited higher d_{ave} and W_{real} values with the increase in d_c being greater than the decrease in d_a (Qiao et al., 2017) (**Fig. 4**). We propose that the strong alkaline treatment can more effectively decrease the thickness of amorphous lamellae and increase crystalline lamellae. As a result, there were lower W_{real} values of S-0.5-6 and S-0.5-12 than those of S-0.1-6 and S-0.1-12 (**Fig. 4**).

3.5 Large-scale features

To interrogate the large-scale structures such as growth rings and blocklets, **Table 3** lists the fitted parameters for the two power-law regimes extended to an ultra-small angle (0.00045 $Å^{-1}$). By fitting the data at low q values (below 0.015 $Å^{-1}$), power law scattering, with an exponent consistent with surface fractal behaviour ($\delta_1 > 3$), was observed for the starch without or with alkaline treatment, with a Guinier scattering from a structure with a radius of gyration (R_{g1}). R_{g1} ranges from 326 to 343 nm, corresponding to a diameter of about 1 µm by assuming spherical objects (Beaucage, Kammler, & Pratsinis, 2004), which could be related to larger blocklets or growth rings with finite roughness (Gallant, Bouchet, & Baldwin, 1997). Larger 'blocklets' have been proposed in the hard semicrystalline rings of the starch granule with smaller blocklets in the softer amorphous rings (Gallant et al., 1997; Pérez, Baldwin, & Gallant, 2009; Pérez & Bertoft, 2010). The length of a blocklet has also been purported to correspond to the length of a single amylopectin molecule (Szymońska & Krok, 2003). In **Table 3**, no statistically apparent changes in R_{g1} by alkaline treatment could be found. The 0.1% (w/v) alkaline treatment did not change δ_1 and the 0.5% (w/v) alkaline

334 solution only reduced δ_1 slightly (especially for S-0.5-6). Structures at these larger length scales were
335 hardly altered by the alkaline conditions used in this work, irrespective of strength or time.

336

337 **Table 3** Fitted parameters for the SANS data in the low *q* range (1st level) and in the high *q* range (2nd
338 level) for waxy maize starch subjected to 0.1% (w/v) NaOH or 0.5% (w/v) NaOH solution treatment
339 for 6 or 12 days [a]

	S	S-0.1-6	S-0.1-12	S-0.5-6	S-0.5-12
G_1 (10^5)	1.59±0.35	1.79±0.41	1.84±0.43	0.98±0.22	1.55±0.36
R_{g1} (nm)	342.5±13.7	342.0±13.6	339.2±13.8	326.2±13.9	342.8±15.7
C_1 (10^{-7})	1.46±0.33	1.01±0.23	1.04±0.24	5.92±1.54	3.32±0.71
δ_1	3.40±0.04	3.46±0.04	3.46±0.04	3.15±0.04	3.30±0.03
G_2	0.93±0.18	0.91±0.24	0.93±0.17	1.51±0.16	1.57±0.20
R_{g2} (nm)	12.8±1.37	13.1±1.9	12.5±1.4	12.0±0.8	11.9±1.0
C_2 (10^{-4})	3.59±1.90	3.79±2.37	3.06±1.58	1.15±0.44	1.69±0.71
δ_2	1.68±0.14	1.65±0.17	1.74±0.14	2.16±0.11	2.09±0.12

340 [a] 1st level covers *ca*. 0.00045 to 0.015 Å^{-1}; 2nd level covers 0.015 to 0.20 Å^{-1}. Parameters obtained by fitting SANS data with
341 **Eq. (1)**: G_1 and G_2, prefactors of the Guinier scattering for the first- and second-level *q*-ranges, respectively; R_{g1} and R_{g1}, radii
342 of gyration for the first- and second-level *q*-ranges, respectively; C_1 and C_2, prefactors of the power law for the first- and
343 second-level *q*-ranges, respectively; δ_1 and δ_2, power-law exponents for the first- and second-level *q*-ranges, respectively. All
344 the values are represented in average ± standard deviation.

345

In the q range above 0.015 $Å^{-1}$, the untreated starch showed a power-law exponent (δ_2) ranging from 1.60 to 2.20, that may be related to mass fractal structures, and a gyration radius R_{g2} of 12–13 nm. Assuming monodisperse spherical objects of uniform scattering density, R_{g2} corresponds to a diameter of about 40 nm, which is within the size range of small starch blocklets as shown by other methods (Doutch et al., 2013). Blocklet size is reported to vary in location within the granule and with botanical source (Tang, Mitsunaga, & Kawamura, 2006; Pérez et al., 2010). Thus, these two parameters could be associated with the blocklets and/or regions of organisation within the branching structure of growth rings. Here, the 0.1% (w/v) alkaline treatment did not lead to apparent changes in δ_2 whereas there was an increase in δ_2 with the use of 0.5% (w/v) NaOH solution. These differences on length-scales greater than lamellae are apparent in Figure 1D. However, no apparent variation in R_{g2} after either the 0.1% (w/v) or 0.5% (w/v) alkaline treatment could be observed, suggesting little change to the blocklets and/or organisation regions (with R_{g2} of 12–13 nm) within the branching structure of growth rings. Our previous SAXS data showed that the 0.1% (w/v) alkaline treatment had no apparent effect on blocklets and mass fractals (with R_{g2} of *ca.* 195 Å), whereas the 0.5% (w/v) alkaline treatment lead to an increase in R_{g2}, which may be linked to the changes to larger-scale structural features as discussed above.

It should be noted that the absence of structural changes within the extended-q SANS scattering data here only reflects changes on length scales up to about 1 µm. Ultra-small-angle neutron scattering (USANS) can readily provide data about structural changes on even larger scales, corresponding to the alteration to granule morphology caused by alkaline treatment as observed by scanning electron microscopy (SEM) (Wang et al., 2012; Cai et al., 2014; Wang et al., 2014; Qiao et al., 2017). As an example, Yang et al. (Yang et al., 2019b) recently used USANS to study pore size

368 and distribution during amyloglucosidase hydrolysis of corn starch which could be directly
369 correlated with SEM; they noted that USANS provides information on internal pores as well as
370 surface pores. The difference in the large-scale parameters, extracted from unified model fits to the
371 SAXS and SANS data, may arise from scattering contrast sensitivities due to differential solvent
372 accessibility or the different fitted *q* ranges, with the extended-*q* SANS accessing lower *q*.
373

374 ### 3.6 Further discussion

375 Early studies (Wootton & Ho, 1989; Ragheb, Abdel-Thalouth, & Tawfik, 1995) have shown that
376 NaOH solutions of high concentration could cause starch gelatinization. The question is to what
377 extent relatively low concentrations (0.1% and 0.5%, w/v) of NaOH could vary the starch structures
378 without degrading starch molecules. Despite the apparent changes in starch molecular order (double
379 helices) and crystallinity (Qiao et al., 2017), the variations by alkaline treatment at the large-scale
380 structural features (growth rings and blocklets) measured by SAXS and extended-*q* SANS were
381 minor except for the lower overall lamellar ordering (reflected by *A*) exhibited by S-0.5-6. We,
382 therefore, propose the changes caused by NaOH solutions at low concentration start from the
383 smaller-scale structural features (double helices and crystallites), whereas the fundamental
384 arrangement of lamellae, growth rings, and blocklets are largely conserved, at least under the
385 treatment conditions and times studied here. Alkaline treatment may cause slight changes to starch
386 double helices resulting in the slightly increased thickness (d_{ave}) of semicrystalline lamellae, while
387 the lamellar ordering was mostly not varied. Only S-0.5-6 displayed a reduced degree of the lamellar
388 ordering. Regarding this, the 0.5% (w/v) alkaline treatment may initially lead to a crystalline

smectic–nematic transition in some parts of crystalline lamellae (similar to the case of starch gelatinization with limited water (Waigh et al., 2000a; Waigh, Kato, Donald, Gidley, Clarke, & Riekel, 2000b)). However, a longer time of alkaline treatment could bring the double helices back to a smectic state so a restored *A* value for S-0.5-12 was observed. The latter nematic-smectic transition should be contributed by the small-scale changes such as the enhanced order of starch double helices. These proposed changes are illustrated in **Fig. 5**, which shows the mild alkaline conditions primarily impact small-scale structural features.

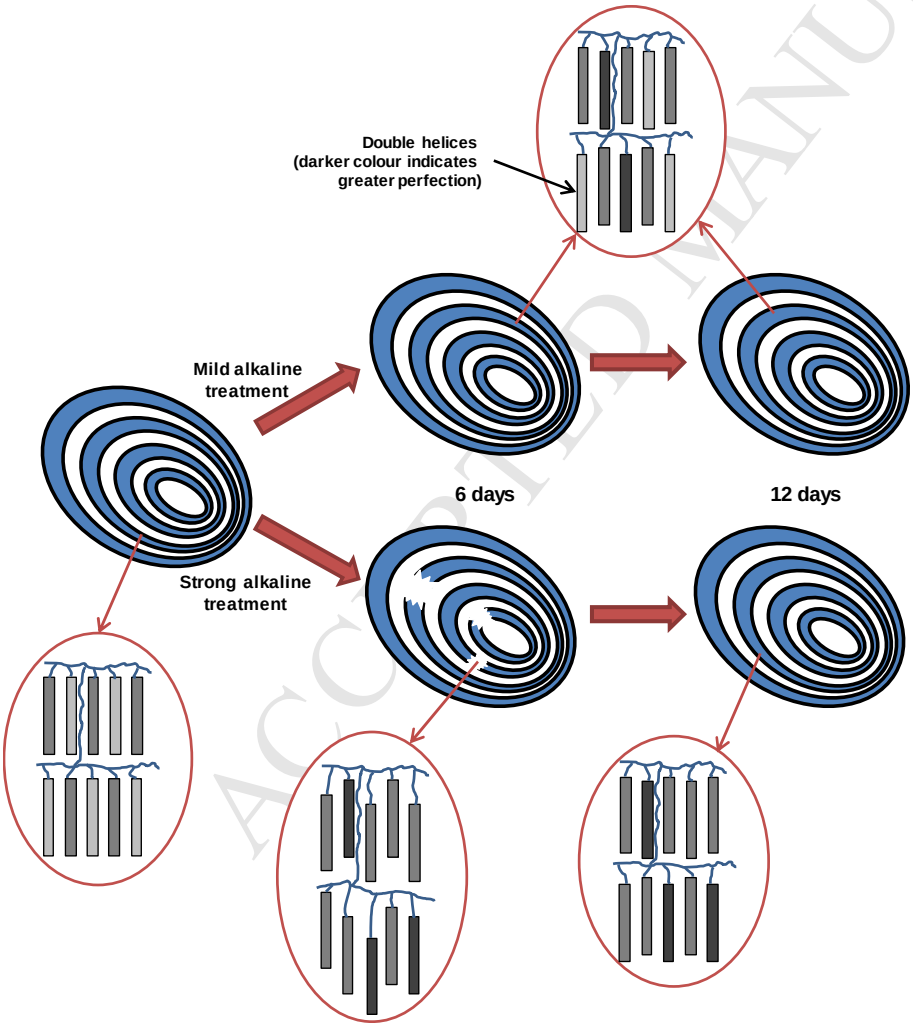

Fig. 5. Schematic representation of the changes in starch lamellar structure and molecular order by alkaline treatment.

The patterns of change to waxy maize starch subjected to alkaline treatment is clearly different from those suffered by other types of starch. An early study (Cardoso et al., 2007) has indicated that the granule organisation of rice starch could be significantly altered with NaOH solutions of concentrations higher than 0.24% (w/v). In a study of C-type starch granules (Thys et al., 2008), SAXS analysis indicated a gradual compression of the semicrystalline growth rings through the swelling of the amorphous growth rings, while wide-angle X-ray scattering indicated a partial degradation of B-type allomorph of starch when granules were alkali-treated. Cai et al. (2014) reported that the treatment of starch by 0.1% (w/v) or 0.4% (w/v) NaOH solution for up to 14 days decreased the difference in electron density between crystalline and amorphous lamellae of starch. Despite these, in these previous studies (Cai et al., 2014; Wang et al., 2014), the changes in amylose content and crystalline structure including long- and short-range ordered structure and crystallinity were not pronounced. As the susceptibility of starch to different physical and chemical treatments highly depends on its native granule architecture and molecular structure, it is always relevant to explore the mechanisms behind these starch structural changes caused by these different treatments.

Our previous study (Qiao et al., 2017) has shown significant changes to the starch digestion behaviour caused by the same alkaline conditions. Taking the results from extended-*q* SANS into consideration, the varied digestion behaviour of waxy maize starch could be mainly linked to the changes in the small-scale structures (starch molecular order and crystallites) whereas the large-scale structural features (lamellae, growth rings, and blocklets) contributes little.

4. Conclusions

Using extended-*q* SANS, in concert with other complementary characterisation techniques, and spanning length-scales from the nanometer to micron, our work has revealed the extent of structural changes on multiple length scales of waxy maize starch subjected to mild alkaline treatment. For this A-type polymorphic starch containing mostly amylopectin, we found the action of either the 0.1% (w/v) or 0.5% (w/v) alkaline solution occurs at the smaller length-scale (i.e. starch double helices and crystallites), whereas the large-scale structural motifs such as lamellae, growth rings and blocklets were largely conserved. This approach and the information gained can provide insights into the rational design of granular starch products with varied functions as well as process optimisation.

Acknowledgments

The authors would like to acknowledge the National Natural Science Foundation of China (NSFC) (Project Nos. 31701637 and 31801582), the Fundamental Research Funds for the Central Universities (Project No. 2662016QD008), the China Postdoctoral Science Foundation (Project No. 2018M642865), the Department of Education, Hubei Province (Q20181407), and the Doctoral Startup Foundation, Hubei University of Technology (BSQD2016024). B. Zhang also would like to thank for the supports from the Young Elite Scientists Sponsorship Program of the China Association for Science and Technology, the Chutian Scholars Program of Hubei Province, and the Shishan Scholars Program of Huazhong Agricultural University. F. Xie acknowledges the support from the European Union's Horizon 2020 research and innovation programme under the Marie Skłodowska-Curie grant agreement No. 798225. D. Wang thanks for the support from the Australian

Research Council (ARC) under a Discovery Project (Project No. DP190101734). This research was undertaken on the QUOKKA instrument at the OPAL reactor at the Australian Nuclear Science and Technology Organisation (ANSTO), New South Wales, Australia.

References

Bai, Y., Cai, L., Doutch, J., Gilbert, E. P., & Shi, Y.-C. (2014). Structural changes from native waxy maize starch granules to cold-water-soluble pyrodextrin during thermal treatment. *Journal of Agricultural and Food Chemistry*, 62, 4186-4194.

Beaucage, G. (2004). Determination of branch fraction and minimum dimension of mass-fractal aggregates. *Physical Review E*, 70, 031401.

Beaucage, G., Kammler, H., & Pratsinis, S. (2004). Particle size distributions from small-angle scattering using global scattering functions. *Journal of applied crystallography*, 37, 523-535.

Bertoft, E., & Manelius, R. (1992). A method for the study of the enzymic hydrolysis of starch granules. *Carbohydrate research*, 227, 269-283.

Blazek, J., & Gilbert, E. P. (2010). Effect of enzymatic hydrolysis on native starch granule structure. *Biomacromolecules*, 11, 3275-3289.

Blazek, J., & Gilbert, E. P. (2011). Application of small-angle x-ray and neutron scattering techniques to the characterisation of starch structure: A review. *Carbohydrate Polymers*, 85, 281-293.

Buleon, A., Colonna, P., Planchot, V., & Ball, S. (1998). Starch granules: Structure and biosynthesis. *Int J Biol Macromol*, 23, 85-112.

463 Cai, J., Yang, Y., Man, J., Huang, J., Wang, Z., Zhang, C., Gu, M., Liu, Q., & Wei, C. (2014).
464 Structural and functional properties of alkali-treated high-amylose rice starch. *Food*
465 *Chemistry*, 145, 245-253.
466 Campus-Baypoli, O. N., Rosas-Burgos, E. C., Torres-Chavez, P. I., Ramírez-Wong, B., &
467 Serna-Saldivar, S. O. (1999). Physiochemical changes of starch during maize tortilla
468 production. *Starch-Starke*, 51, 173-176.
469 Cardoso, M. B., Putaux, J.-L., Samios, D., & da Silveira, N. P. (2007). Influence of alkali
470 concentration on the deproteinization and/or gelatinization of rice starch. *Carbohydrate*
471 *Polymers*, 70, 160-165.
472 Cardoso, M. B., & Westfahl, H. (2010). On the lamellar width distributions of starch. *Carbohydrate*
473 *Polymers*, 81, 21-28.
474 Chanvrier, H., Appelqvist, I. A. M., Bird, A. R., Gilbert, E., Htoon, A., Li, Z., Lillford, P. J.,
475 Lopez-Rubio, A., Morell, M. K., & Topping, D. L. (2007). Processing of novel elevated
476 amylose wheats: Functional properties and starch digestibility of extruded products. *Journal*
477 *of Agricultural and Food Chemistry*, 55, 10248-10257.
478 Correia, P. R., & Beirão-da-Costa, M. L. (2012). Starch isolation from chestnut and acorn flours
479 through alkaline and enzymatic methods. *Food and Bioproducts Processing*, 90, 309-316.
480 Doutch, J., & Gilbert, E. P. (2013). Characterisation of large scale structures in starch granules via
481 small-angle neutron and x-ray scattering. *Carbohydrate Polymers*, 91, 444-451.
482 Flanagan, B. M., Gidley, M. J., & Warren, F. J. (2015). Rapid quantification of starch molecular
483 order through multivariate modelling of 13c cp/mas nmr spectra. *Chemical Communications*,
484 51, 14856-14858.

485 Fuentes-Zaragoza, E., Sánchez-Zapata, E., Sendra, E., Sayas, E., Navarro, C., Fernández-López, J.,
486 & Pérez-Alvarez, J. A. (2011). Resistant starch as prebiotic: A review. *Starch-Stärke*, 63,
487 406-415.
488 Gallant, D. J., Bouchet, B., & Baldwin, P. M. (1997). Microscopy of starch: Evidence of a new level
489 of granule organization. *Carbohydrate Polymers*, 32, 177-191.
490 Gilbert, E. P., Schulz, J. C., & Noakes, T. J. (2006). 'Quokka'—the small-angle neutron scattering
491 instrument at opal. *Physica B: Condensed Matter*, 385-386, 1180-1182.
492 Han, J.-A., & Lim, S.-T. (2004). Structural changes in corn starches during alkaline dissolution by
493 vortexing. *Carbohydrate Polymers*, 55, 193-199.
494 Han, X. Z., & Hamaker, B. R. (2002). Partial leaching of granule-associated proteins from rice starch
495 during alkaline extraction and subsequent gelatinization. *Starch-Stärke*, 54, 454-460.
496 Jiang, Q., Gao, W., Li, X., Man, S., Shi, Y., Yang, Y., Huang, L., & Liu, C. (2014). Comparative
497 susceptibilities to alkali-treatment of a-, b- and c-type starches of dioscorea zingiberensis,
498 dioscorea persimilis and dioscorea opposita. *Food Hydrocolloids*, 39, 286-294.
499 Jiang, Q. Q., Gao, W. Y., Li, X., & Zhang, J. Z. (2011). Characteristics of native and enzymatically
500 hydrolyzed zea mays l., fritillaria ussuriensis maxim. And dioscorea opposita thunb. Starches.
501 *Food Hydrocolloids*, 25, 521-528.
502 Juansang, J., Puttanlek, C., Rungsardthong, V., Puncha-arnon, S., & Uttapap, D. (2012). Effect of
503 gelatinisation on slowly digestible starch and resistant starch of heat-moisture treated and
504 chemically modified canna starches. *Food Chemistry*, 131, 500-507.

505 Karim, A. A., Nadiha, M. Z., Chen, F. K., Phuah, Y. P., Chui, Y. M., & Fazilah, A. (2008). Pasting
506 and retrogradation properties of alkali-treated sago (metroxylon sagu) starch. *Food*
507 *Hydrocolloids*, 22, 1044-1053.
508 Lai, L., Karim, A. A., Norziah, M., & Seow, C. (2002). Effects of na_2co_3 and naoh on dsc thermal
509 profiles of selected native cereal starches. *Food chemistry*, 78, 355-362.
510 Liu, H., Xie, F., Yu, L., Chen, L., & Li, L. (2009). Thermal processing of starch-based polymers.
511 *Progress in Polymer Science*, 34, 1348-1368.
512 Liu, W. C., Halley, P. J., & Gilbert, R. G. (2010). Mechanism of degradation of starch, a highly
513 branched polymer, during extrusion. *Macromolecules*, 43, 2855-2864.
514 Lopez-Rubio, A., Flanagan, B. M., Gilbert, E. P., & Gidley, M. J. (2008a). A novel approach for
515 calculating starch crystallinity and its correlation with double helix content: A combined xrd
516 and nmr study. *Biopolymers*, 89, 761-8.
517 Lopez-Rubio, A., Flanagan, B. M., Shrestha, A. K., Gidley, M. J., & Gilbert, E. P. (2008b).
518 Molecular rearrangement of starch during in vitro digestion: Toward a better understanding of
519 enzyme resistant starch formation in processed starches. *Biomacromolecules*, 9, 1951-8.
520 Lopez-Rubio, A., Htoon, A., & Gilbert, E. P. (2007). Influence of extrusion and digestion on the
521 nanostructure of high-amylose maize starch. *Biomacromolecules*, 8, 1564-1572.
522 Luengwilai, K., & Beckles, D. M. (2009). Structural investigations and morphology of tomato fruit
523 starch. *J Agric Food Chem*, 57, 282-91.
524 Méndez-Montealvo, G., Trejo-Espino, J. L., Paredes-López, O., & Bello-Pérez, L. A. (2007).
525 Physicochemical and morphological characteristics of nixtamalized maize starch. *Starch -*
526 *Stärke*, 59, 277-283.

527 Noda, T., Takigawa, S., Matsuura-Endo, C., Suzuki, T., Hashimoto, N., Kottearachchi, N. S.,
528 Yamauchi, H., & Zaidul, I. S. M. (2008). Factors affecting the digestibility of raw and
529 gelatinized potato starches. *Food Chemistry*, 110, 465-470.
530 Nor Nadiha, M. Z., Fazilah, A., Bhat, R., & Karim, A. A. (2010). Comparative susceptibilities of
531 sago, potato and corn starches to alkali treatment. *Food Chemistry*, 121, 1053-1059.
532 Pérez, S., Baldwin, P. M., & Gallant, D. J. (2009). Structural features of starch granules i. In B.
533 James, & W. Roy, *Starch (third edition)* (pp. 149-192). San Diego: Academic Press.
534 Perez, S., & Bertoft, E. (2010). The molecular structures of starch components and their contribution
535 to the architecture of starch granules: A comprehensive review. *Starch-Starke*, 62, 389-420.
536 Pérez, S., & Bertoft, E. (2010). The molecular structures of starch components and their contribution
537 to the architecture of starch granules: A comprehensive review. *Starch/Stärke*, 62, 389-420.
538 Pikus, S. (2005). Small-angle x-ray scattering (saxs) studies of the structure of starch and starch
539 products. *Fibres and Textiles in Eastern Europe*, 13, 82-86.
540 Praznik, W., Buksa, K., Ziobro, R., Gambuś, H., & Nowotna, A. (2012). The effect of long-term
541 alkali treatment on the molecular characteristics of native and extruded starches at 35° c.
542 *Starch-Stärke*, 64, 890-897.
543 Pu, H., Chen, L., Li, X., Xie, F., Yu, L., & Li, L. (2011). An oral colon-targeting controlled release
544 system based on resistant starch acetate: Synthetization, characterization, and preparation of
545 film-coating pellets. *Journal of Agricultural and Food Chemistry*, 59, 5738-5745.
546 Qiao, D., Xie, F., Zhang, B., Zou, W., Zhao, S., Niu, M., Lv, R., Cheng, Q., Jiang, F., & Zhu, J.
547 (2017). A further understanding of the multi-scale supramolecular structure and digestion rate
548 of waxy starch. *Food Hydrocolloids*, 65, 24-34.

549 Qiao, D., Yu, L., Liu, H., Zou, W., Xie, F., Simon, G., Petinakis, E., Shen, Z., & Chen, L. (2016).
550 Insights into the hierarchical structure and digestion rate of alkali-modulated starches with
551 different amylose contents. *Carbohydrate Polymers*, 144, 271-281.
552 Ragheb, A. A., Abdel-Thalouth, I., & Tawfik, S. (1995). Gelatinization of starch in aqueous alkaline
553 solutions. *Starch - Stärke*, 47, 338-345.
554 Shrestha, A. K., Blazek, J., Flanagan, B. M., Dhital, S., Larroque, O., Morell, M. K., Gilbert, E. P., &
555 Gidley, M. J. (2015). Molecular, mesoscopic and microscopic structure evolution during
556 amylase digestion of extruded maize and high amylose maize starches. *Carbohydrate*
557 *Polymers*, 118, 224-234.
558 Situ, W., Li, X., Liu, J., & Chen, L. (2015). Preparation and characterization of glycoprotein-resistant
559 starch complex as a coating material for oral bioadhesive microparticles for colon-targeted
560 polypeptide delivery. *Journal of Agricultural and Food Chemistry*, 63, 4138-4147.
561 Szymońska, J., & Krok, F. (2003). Potato starch granule nanostructure studied by high resolution
562 non-contact afm. *International Journal of Biological Macromolecules*, 33, 1-7.
563 Tan, I., Flanagan, B. M., Halley, P. J., Whittaker, A. K., & Gidley, M. J. (2007). A method for
564 estimating the nature and relative proportions of amorphous, single, and double-helical
565 components in starch granules by ^{13}c cp/mas nmr. *Biomacromolecules*, 8, 885-891.
566 Tang, H., Mitsunaga, T., & Kawamura, Y. (2006). Molecular arrangement in blocklets and starch
567 granule architecture. *Carbohydrate Polymers*, 63, 555-560.
568 Thys, R. C. S., Westfahl, H., Norea, C. P. Z., Marczak, L. D. F., Silveira, N. P., & Cardoso, M. B.
569 (2008). Effect of the alkaline treatment on the ultrastructure of c-type starch granules.
570 *Biomacromolecules*, 9, 1894-1901.

Waigh, T. A., Gidley, M. J., Komanshek, B. U., & Donald, A. M. (2000a). The phase transformations in starch during gelatinisation: A liquid crystalline approach. *Carbohydrate Research*, 328, 165-176.

Waigh, T. A., Kato, K. L., Donald, A. M., Gidley, M. J., Clarke, C. J., & Riekel, C. (2000b). Side-chain liquid-crystalline model for starch. *Starch/Stärke*, 52, 450-460.

Wang, H., Wang, Z., Li, X., Chen, L., & Zhang, B. (2017). Multi-scale structure, pasting and digestibility of heat moisture treated red adzuki bean starch. *International Journal of Biological Macromolecules*, 102, 162-169.

Wang, S., & Copeland, L. (2012). Effect of alkali treatment on structure and function of pea starch granules. *Food Chemistry*, 135, 1635-1642.

Wang, S., Luo, H., Zhang, J., Zhang, Y., He, Z., & Wang, S. (2014). Alkali-induced changes in functional properties and in vitro digestibility of wheat starch: The role of surface proteins and lipids. *Journal of Agricultural and Food Chemistry*, 62, 3636-3643.

Witt, T., Doutch, J., Gilbert, E. P., & Gilbert, R. G. (2012). Relations between molecular, crystalline, and lamellar structures of amylopectin. *Biomacromolecules*, 13, 4273-4282.

Wood, K., Mata, J. P., Garvey, C. J., Wu, C.-M., Hamilton, W. A., Abbeywick, P., Bartlett, D., Bartsch, F., Baxter, P., Booth, N., Brown, W., Christoforidis, J., Clowes, D., d'Adam, T., Darmann, F., Deura, M., Harrison, S., Hauser, N., Horton, G., Federici, D., Franceschini, F., Hanson, P., Imamovic, E., Imperia, P., Jones, M., Kennedy, S., Kim, S., Lam, T., Lee, W. T., Lesha, M., Mannicke, D., Noakes, T., Olsen, S. R., Osborn, J. C., Penny, D., Perry, M., Pullen, S. A., Robinson, R. A., Schulz, J. C., Xiong, N., & Gilbert, E. P. (2018). Quokka, the pinhole small-angle neutron scattering instrument at the opal research reactor, australia: Design,

performance, operation and scientific highlights. *Journal of Applied Crystallography*, 51, 294-314.

Wootton, M., & Ho, P. (1989). Alkali gelatinisation of wheat starch. *Starch - Stärke*, 41, 261-265.

Xie, F., Halley, P. J., & Avérous, L. (2012). Rheology to understand and optimize processibility, structures and properties of starch polymeric materials. *Progress in Polymer Science*, 37, 595-623.

Xie, F., Zhang, B., & Wang, D. K. (2017). Chapter 7 - starch thermal processing: Technologies at laboratory and semi-industrial scales. In M. A. Villar, S. E. Barbosa, M. A. García, L. A. Castillo, & O. V. López, *Starch-based materials in food packaging* (pp. 187-227). Academic Press.

Yang, Z., Xu, X., Singh, R., de Campo, L., Gilbert, E. P., Wu, Z., & Hemar, Y. (2019a). Effect of amyloglucosidase hydrolysis on the multi-scale supramolecular structure of corn starch. *Carbohydrate Polymers*, In press.

Yang, Z., Xu, X., Singh, R., de Campo, L., Gilbert, E. P., Wu, Z., & Hemar, Y. (2019b). Effect of amyloglucosidase hydrolysis on the multi-scale supramolecular structure of corn starch. *Carbohydrate Polymers*, 212, 40-50.

Zhang, B., Chen, L., Xie, F., Li, X., Truss, R. W., Halley, P. J., Shamshina, J. L., Rogers, R. D., & McNally, T. (2015). Understanding the structural disorganization of starch in water-ionic liquid solutions. *Physical Chemistry Chemical Physics*, 17, 13860-13871.

Zhang, B., Xie, F., Shamshina, J. L., Rogers, R. D., McNally, T., Halley, P. J., Truss, R. W., Chen, L., & Zhao, S. (2017a). Dissolution of starch with aqueous ionic liquid under ambient conditions. *ACS Sustainable Chemistry & Engineering*, 5, 3737-3741.

615 Zhang, B., Xie, F., Shamshina, J. L., Rogers, R. D., McNally, T., Wang, D. K., Halley, P. J., Truss, R.
616 W., Zhao, S., & Chen, L. (2017b). Facile preparation of starch-based electroconductive films
617 with ionic liquid. *ACS Sustainable Chemistry & Engineering*, 5, 5457-5467.
618 Zhang, B., Zhao, Y., Li, X., Zhang, P., Li, L., Xie, F., & Chen, L. (2014). Effects of amylose and
619 phosphate monoester on aggregation structures of heat-moisture treated potato starches.
620 *Carbohydrate Polymers*, 103, 228-233.
621

Highlights:

- ✓ Extended-*q* SANS detects larger-scale structural changes of waxy maize starch
- ✓ Mild alkaline treatment mainly changes starch double helices and crystallites
- ✓ Lamellar and supramolecular structures were conserved during the alkaline treatment
- ✓ There were minimal changes at larger scales (e.g., blocklets and growth rings)
- ✓ The mechanism of mild alkaline treatment of waxy maize starch is revealed